Phase-resolved gamma-ray spectroscopy of LS 5039. (COST-STSM-MP1304-34549)

1 Introduction

LS 5039 is one of the few known γ-ray binaries in the Galaxy. All these systems belong to the high-mass X-ray binary (HMXB) population, but they are peculiar examples of the HMXBs with the energy output dominated by emission in the high-energy (GeV) γ-ray band. The nature of this peculiarity is not completely understood yet. At least one system, PSR B1259-63 is known to be powered by a young pulsar (Johnston et al., 1992). The nature of the compact objects orbiting massive stars in other systems is not constrained. However, similarity of the spectral characteristics of the known γ-ray binaries suggests similar nature of the compact objects in these systems (see Dubus (2013) for a review). Presence of the young rotation powered pulsar could potentially also explain the rarity of the γ-ray binaries in the Galaxy. The lifetime of the rotation powered pulsars is relatively short, compared to the lifetime of the classical HMXBs, so that only a small fraction of the youngest HMXBs with neutron stars contain rotation powered pulsars. In the absence of a direct proof of the neutron star nature of the compact object, models assuming the activity powered by accretion onto a black hole could not be discarded (Barkov & Khangulyan, 2012; Owocki, Okazaki & Romero, 2011). Note, that the current knowledge of the mass of the compact object is consistent with both neutron star and black hole possibilities (Sarty et al., 2011; Moldón, Ribó & Paredes, 2012).

The LS 5039 system was classified as a HMXB based on the ROSAT all-sky survey data (Motch et al., 1997). The stellar companion is a bright star with V = 11.2 and its spectral type is O6.5V(f). The distance to the binary is about 2.5 ± 0.1 kpc (Casares et al., 2005). The compact object is orbiting around the stellar companion with an orbital period $P_{orb} \simeq 3.90603$ days and with eccentricity e = 0.35 ± 0.04 (Casares et al., 2005).

LS 5039 is a remarkable system among the γ-ray binaries in the sense that it exhibits very stable X-ray behaviour, with orbital variability properties not changing from orbit to orbit on the time scales of years (Kishishita et al., 2009; Hadasch et al., 2012). Such behaviour might be explained by the stability of the properties of the wind from the massive companion. The orbital period of the system is relatively short, compared to the other γ-ray binaries. This means that the compact object moves close to the surface of the massive star, with the orbital separation at the periastron being just about twice the radius of the O star, growing to four stellar radii at the apastron. The compact object always moves through a densest part of the stellar wind (touching the wind formation / acceleration zone). In such conditions, pulsed radio emission from the putative young pulsar in the system could not be detected because of the strong free-free absorption.

First evidence for high-energy particle acceleration of the system was found based on the observations in the radio band (Marti, Paredes & Ribo, 1998). γ-ray emission from the system was first discovered in the TeV energy band by HESS telescopes (Aharonian et al., 2005). The TeV signal from the system is modulated on the orbital time scale, with a maximum close to the phase of inferior conjunction of the orbit (Aharonian et al., 2006). Suzaku X-ray observations of LS 5039 during the whole orbit shows similar orbital behaviour of the TeV and X-ray emission (Takahashi et al., 2009). To the contrary, the GeV γ-ray emission, detected by *Fermi* reveals a different orbital modulation pattern, with a pronounced maximum at the periastron and a suppression of the flux at the inferior conjunction (Abdo et al., 2009).

Explanation of both variability patterns, as well as of the energy dependence of the variability pattern pro-

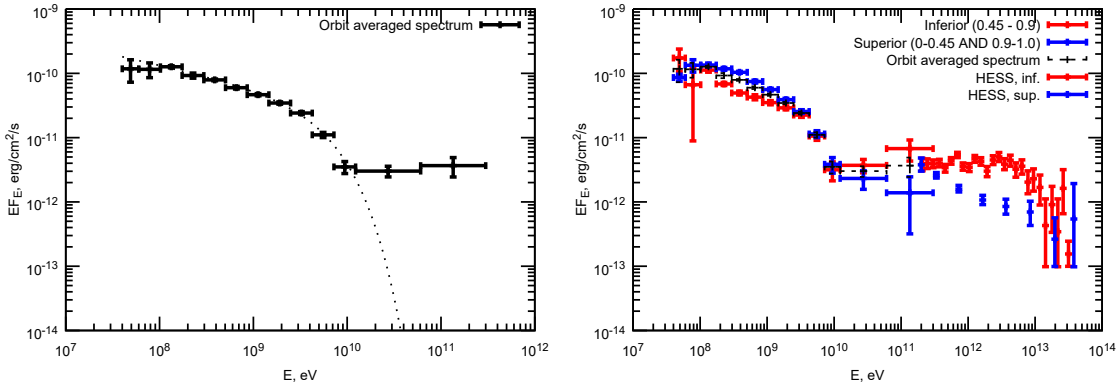

Fig. 1: Spectral energy distribution of LS 5039. *Left panel:* Phase averaged spectrum with the best cut-off powerlaw fits in 0.1-1 GeV energy band from Hadasch (2012)(red dashed curve) and this work(black dashed curve). *Right panel:* Phase resolved LS 5039 spectra for superior (phases 0.0-0.45 and 0.45-0.9) and inferior conjunctions (phases 0.45-0.9) similar to Abdo et al. (2009); Hadasch (2012). HESS data points for the same orbital phases are shown with blue and red points.

vides a challenge for phenomenological models of the source. Several alternative explanations were proposed in the past. In the paper of Takahashi et al. (2009) authors interpret close correlation of the X-ray and TeV gamma-ray light curves as an evidence of production of these two radiation components by the same electron population via synchrotron radiation and inverse Compton (IC) scattering, respectively. In order to explain the X-ray orbital modulation of the emission they assume a dominance of the adiabatic losses over the radiative (synchrotron and IC) losses of electrons. The light curve in gamma rays depends critically, in addition, on effects related to interactions with the optical photons of the companion star. Photon-photon pair production starts to be important above 30 GeV, which explains the difference between the *Fermi* and HESS lightcurves.

In the paper of Zabalza et al. (2013) authors, however, give arguments in favour of two different regions for the production of the GeV and TeV emission, namely the shocks at the head-on collision of the winds and the termination shock, caused by Coriolis forces on scales larger than the binary separation, correspondingly. In the region close to the star the intense stellar photon field destroys most of the very high energy gamma-rays with energies above 40 GeV, while the Coriolis turnover shock is a good candidate for very high energy emitter (see also discussion in Bosch-Ramon et al., 2012). The predictions of the strength of the magnetic field in this model turned out to be much smaller than assumed by Takahashi et al. (2009), which makes the explanation of the observed X-ray orbital modulation more problematic.

In the work of Pétri & Dubus (2011), authors also assume a separate region for the production of the GeV emission, but they propose to locate it very close to the compact object, which they assume to be a hidden pulsar. Namely they study the possibility of the inverse Compton scattering of the optical photons on the relativistic electrons of the striped pulsar wind before the shock.

2 Fermi/LAT results

Fermi/LAT is an instrument on board of γ-ray Fermi satellite. It operates at energies $\sim$ 30 MeV – $\gtrsim$ 300 GeV and covers the whole sky at 3 hours timescale (Atwood et al., 2009).

For the Fermi/LAT analysis we consider 100 months of the data (August, 4th, 2008 – November, 7th, 2016). The analysis was performed with the latest `v10r0p5` Fermi software. We further restrict the analysis to energies 40 MeV –300 GeV at which the energy dispersion correc-

tion can be performed. Proceeding with binned data analysis we select `CLEAN` class photons with `P8R2_CLEAN_V6` instrument response function (IRF), as high-quality selection photons, recommended by Fermi/LAT collaboration for most analysis[1]. In order to cover the broad at low energies FERMI/LAT PSF we selected the radius of the analysis region to be 19°. The model of the region includes standard templates for galactic and extragalactic diffuse backgrounds as well as all sources from 4 years (3FGL) Fermi catalogue, Acero et al. (2015) in the region. This model was fitted to the data using `BinnedAnalysis` python module and the upper limits for the weak sources were calculated by `UpperLimits` module supplied with Fermi software. All upper limits presented in the analysis correspond to 95% confidence range ($\sim 2\sigma$).

Here we used $\sim$ 8 years of Fermi/LAT data that results in $\sim$ 4 times better statistics in comparison with earlier works (Abdo et al., 2009; Hadasch, 2012). The obtained phase-averaged spectrum is consistent with one from Hadasch (2012). Phase averaged spectrum of LS 5039 at energy band 0.04-10 GeV can be described with a cut-off powerlaw model with index $\Gamma = 2.33 \pm 0.03$, cut-off energy $E_{cut} = 4.9 \pm 0.6$ GeV and normalization at 100 MeV $n = (1.35 \pm 0.06) \cdot 10^{-10}$ erg/cm^2/s, see Fig. 1, left. Longer exposure allows us more accurately measure the flux in high energy tail at $\gtrsim$ 10 GeV, which is consistent with HESS flux measurements. Averaged over orbital phases $0.45 - 0.9$ ("inferior conjunction") and $0.0 - 0.45; 0.9 - 1.0$ ("superior conjunction") spectra together with the HESS data for the same orbital phases are shown in Fig. 1, right.

However, the increased exposure time allowed us to analyse the spectrum in more details than it was done in previous works. This can be clearly seen in the orbital folded light curves at different energies are shown in Fig 2. In lowest energy band (40-100 MeV) the light curve demonstrates behaviour similar to X-rays and TeVs energy band, (Kishishita et al., 2009; Aharonian et al., 2005) with the minimum at phase$\sim$ 0.2. At higher energies ($\gtrsim$ 100 MeV) the minimum shifts to phases 0.5 (at 100 MeV–1 GeV) and 0.75 (1–300 GeV) in agreement with Abdo et al. (2009).

The χ^2 of the fit of each light curve with the constant is given in table 1. The variability is significant ($\gtrsim 3\sigma$) in all energy bands, except highest one, 1-10 GeV.

Energy band	χ^2/NDF	Significance, σ
40-100 MeV	28.8/4	4.45
100 MeV-1 GeV	145.9/4	11.5
1-300 GeV	5.0/4	1.1

Tab. 1: χ^2 and significances of the best fit with constant of LS 5039 phase resolved light curves in different energy bands. See also Fig. 2

We also would like to note, that the ratio between maximal and minimal flux along the orbit decreases with energy. For 40-100 MeV this ratio is 2.6, while it is $\simeq$ 2.1 for 0.1-1 GeV and $\sim$ 1.5 for 1–300 GeV band.

[1] See e.g. http://fermi.gsfc.nasa.gov/ssc/data/analysis/documentation/Cicerone/Cicerone_LAT_IRFs/IRF_overview.html

References

Abdo A. A., Ackermann M., Ajello M., Atwood W. B., Axelsson M., Baldini L., Ballet, 2009, ApJ, 706, L56

Acero F. et al., 2015, ApJS, 218, 23

Aharonian F., Akhperjanian A. G., Aye K.-M., Bazer-Bachi A. R., Beilicke M., Benbow, 2005, Science, 309, 746

Aharonian F. et al., 2006, A&A, 460, 743

Atwood W. B. et al., 2009, ApJ, 697, 1071

Barkov M. V., Khangulyan D. V., 2012, MNRAS, 421, 1351

Bosch-Ramon V., Barkov M. V., Khangulyan D., Perucho M., 2012, A&A, 544, A59

Casares J., Ribó M., Ribas I., Paredes J. M., Martí J., Herrero A., 2005, MNRAS, 364, 899

Dubus G., 2013, A&A Rev., 21, 64

Hadasch D., 2012, International Journal of Modern Physics Conference Series, 8, 61

Hadasch D. et al., 2012, ApJ, 749, 54

Johnston S., Manchester R. N., Lyne A. G., Bailes M., Kaspi V. M., Qiao G., D'Amico N., 1992, ApJ, 387, L37

Kishishita T., Tanaka T., Uchiyama Y., Takahashi T., 2009, ApJ, 697, L1

Marti J., Paredes J. M., Ribo M., 1998, A&A, 338, L71

Moldón J., Ribó M., Paredes J. M., 2012, A&A, 548, A103

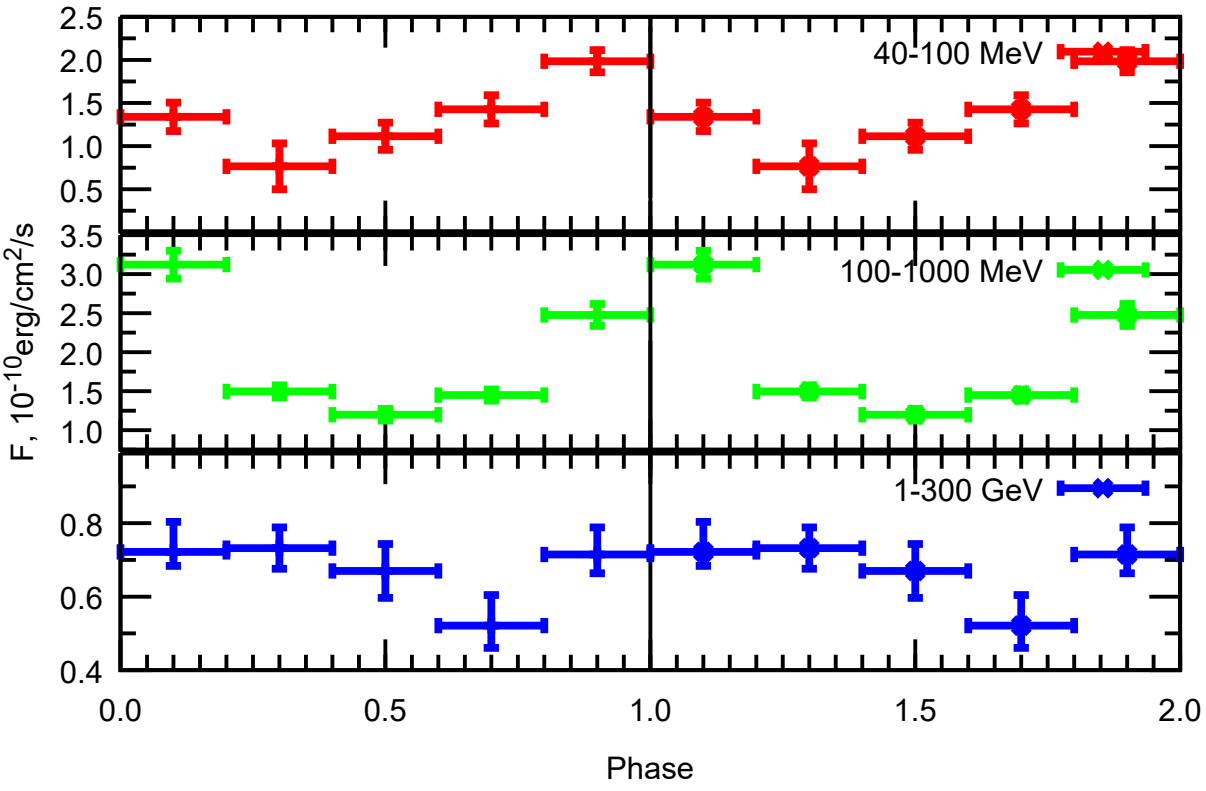

Fig. 2: Orbital-folded lightcurve of LS 5039 in different energy bands: 40-100 MeV (top), 100 MeV–1 GeV (middle) and 1-300 GeV (bottom). In lowest energy band (40-100 MeV) the light curve demonstrates behaviour similar to X-rays and TeVs energy band, (Kishishita et al., 2009; Aharonian et al., 2005) with the minimum at phase$\sim$ 0.2. At higher energies ($\gtrsim$ 100 MeV) the minimum shifts to phases 0.5 (at 100 MeV–1 GeV) and 0.75 (1–300 GeV) in agreement with Abdo et al. (2009).

Motch C., Haberl F., Dennerl K., Pakull M., Janot-Pacheco E., 1997, A&A, 323, 853
Owocki S. P., Okazaki A. T., Romero G., 2011, in IAU Symposium, Vol. 272, IAU Symposium, Neiner C., Wade G., Meynet G., Peters G., eds., pp. 587–592
Pétri J., Dubus G., 2011, MNRAS, 417, 532
Sarty G. E. et al., 2011, MNRAS, 411, 1293
Takahashi T. et al., 2009, ApJ, 697, 592
Zabalza V., Bosch-Ramon V., Aharonian F., Khangulyan D., 2013, A&A, 551, A17